Titanium-doped indium oxide: A high-mobility transparent conductor

M. F. A. M. van Hest, M. S. Dabney, J. D. Perkins, D. S. Ginley, and M. P. Taylor

Citation: Applied Physics Letters **87**, 032111 (2005); doi: 10.1063/1.1995957
View online: http://dx.doi.org/10.1063/1.1995957
View Table of Contents: http://scitation.aip.org/content/aip/journal/apl/87/3?ver=pdfcov
Published by the AIP Publishing

Titanium-doped indium oxide: A high-mobility transparent conductor

M. F. A. M. van Hest,[a] M. S. Dabney, J. D. Perkins, and D. S. Ginley
National Renewable Energy Laboratory, 1617 Cole Boulevard, Golden, Colorado 80401

M. P. Taylor
Colorado School of Mines, Golden, Colorado 80401

(Received 18 February 2005; accepted 2 June 2005; published online 15 July 2005)

We report on the effects of titanium doping (0–7 at. %) on the optical and electrical properties of In_2O_3 using combinatorial deposition and analysis techniques. Maximum mobilities are observed at Ti concentrations of 1.5–2.5 at. % and are $>80\ cm^2/V\,s$ in sputtered films. The carrier concentration increased with titanium content to a high of $8.0\times10^{20}\ cm^{-3}$. Data show that one carrier is generated per added Ti between 1 and 3 at. %. Conductivities up to 6260 $\Omega^{-1}\ cm^{-1}$ were observed. These remained very high $>5000\ \Omega^{-1}\ cm^{-1}$ across a wide compositional range. The optical transparency is high (>85%) in a wide spectral range from 400 nm to at least 1750 nm. The work function of titanium-doped indium oxide varies substantially over the studied compositional range. © *2005 American Institute of Physics*. [DOI: 10.1063/1.1995957]

Transparent conductive oxides (TCOs) are key components in flat-panel displays, photovoltaic cells, smart windows, light-emitting diodes, and optical waveguides.[1] There is an increasing interest in TCOs with high mobility (μ) to increase electrical conductivity (σ) without sacrificing optical transparency. According to the Drude model, increasing the conductivity without compromising the transparency can only be obtained by increasing the mobility. Alternatively, to increase the transparency window without compromising the conductivity, the carrier concentration needs to be decreased while the mobility is increased. Clearly, there is a twofold need for high-mobility materials.

Tin-doped indium oxide (ITO) is a key commercial TCO currently used because of its good optical and electrical properties[2–4] (i.e., Colorado Concept Coatings; σ: 6200 $\Omega^{-1}\ cm^{-1}$; μ: 29 $cm^2\ V^{-1}\ s^{-1}$; N: $1.3\times10^{21}\ cm^{-3}$; λ_p; 1.15 μm). It has been shown over the past four year that using molybdenum instead of tin produces a TCO material with very high carrier mobility ($\sim$70 $cm^2\ V^{-1}\ s^{-1}$).[5–8] More recently, Delahoy *et al.* have shown that doping indium oxide with titanium can improve the electrical and optical properties relative to typical ITO.[9] The results of Delahoy *et al.* were better than those obtained in earlier studies.[10,11]

In this work, we report on a combinatorial investigation of titanium as a dopant in indium oxide. Unlike the case of molybdenum or tin, one carrier is generated for every titanium for doping concentrations between 1 and 3 at. %, therefore making it a significantly better dopant. A maximum in the mobility of 83.3 $cm^2\ V^{-1}\ s^{-1}$ and conductivity of 6260 $\Omega^{-1}\ cm^{-1}$ have been observed for titanium doping of 1.7 and 2.8 at. %, respectively, in combinatorial samples. This is the first study on the dependence of the optoelectronic properties of titanium-doped indium oxide as function of titanium doping concentration.

Combinatorial libraries were deposited by cosputtering of a Ti-doped In_2O_3 and pure In_2O_3 targets. The sputtering system consists of a vacuum bell-jar reactor (Perkin-Elmer A-RCS) with two 2 in.-sputtering guns on either side of the substrate at roughly 45° to the center line. This produces a thickness gradient in the deposited films from each gun and therefore a compositional gradient when films are cosputtered. The sputtering guns are positioned so that the compositional gradient is only in one direction across the sample. The system is cryopumped with a base pressure of less than 1×10^{-6} Torr. The stationary substrate holder can be heated to over 900 °C resistively. A similar setup has been discussed previously for deposition of indium zinc oxide[12] and $Cr_{1-x}Ti_xN_y$.[13] For this study, libraries were sputtered from a pure In_2O_3 (99.99%) target and a 9 wt. % TiO_2 in In_2O_3 (99.99%) target onto 2 in.×2 in. Corning 1737 glass substrates at 550 °C. Films were sputtered in pure argon (grade 5.0) at a flow rate of 20 sccm and a system pressure of 4.5 mTorr. By varying the rf-sputtering powers on the two targets, the TiO_2 content in the films could be varied in the range from 0 to 5 wt. % in as little as three libraries. This is equal to a range from 0 to 7 at. % titanium for indium excluding oxygen. For the results presented here, the power for the pure In_2O_3 target was kept constant at 30 W and the power for the Ti-doped In_2O_3 target was 2, 10, or 20 W. The standard deposition time was 1 h and the thickness of the deposited films was between 200 and 400 nm with a thickness variation across the library of 50 to 150 nm depending on sputtering conditions.

The electrical properties (Hall probe in van der Pauw configuration), elemental composition [electron probe microanalysis (EPMA)], optical transmission and reflection (dispersive grating CCD/GaInAs spectrometer 300 nm–2 μm and Fourier transform infrared (FTIR) spectrometer 2–25 μm), crystal structure [x-ray diffraction (XRD) with two dimensional detector], and work function (contact potential measurement by Kelvin probe) of the deposited libraries have been studied. For measurement purposes, the libraries were virtually divided into four rows each consisting of 11 columns. Since the samples only have a compositional gradient in one direction, the four rows are essentially the same. For the Hall probe measurements a single row is cut into five equally sized pieces. Due to the limited compositional gradient (<3 at. %) along a library, the compositional gradient along one of the five pieces is small (<0.6 at. %), and therefore each piece is considered a single composition sample.

[a]Electronic mail: maikel_van_hest@nrel.gov

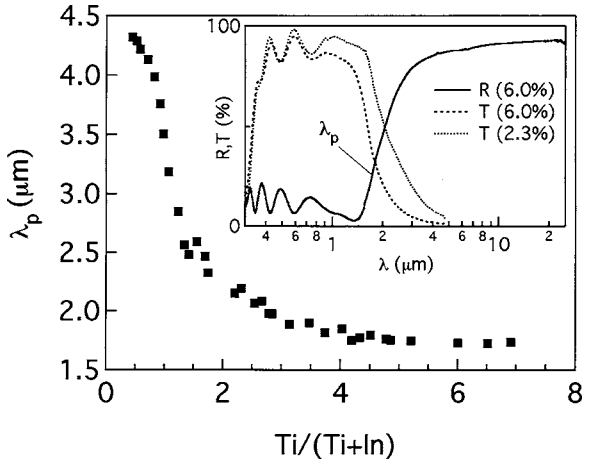

FIG. 1. Plasma wavelength (λ_p) as function of titanium content. Inset: reflection and transmission spectra for a 6.0 at. % Ti-doped In_2O_3 film.

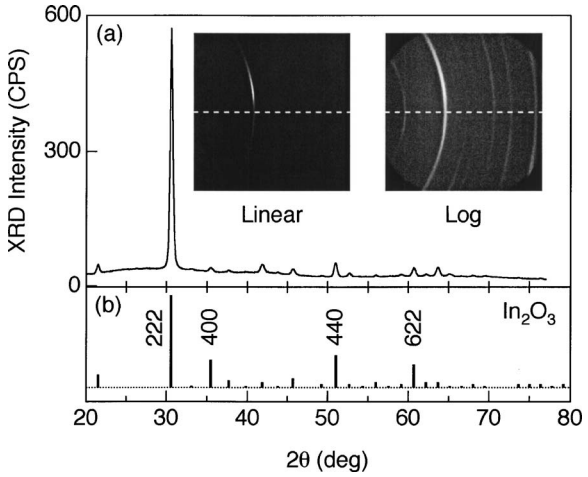

FIG. 2. (a) XRD 2θ spectra of Ti-doped In_2O_3 (2.8 at. %) with the XRD detector frame and (b) the expected XRD peak locations for pure In_2O_3.

More information on the analysis tools can be found elsewhere.[12–14]

Figure 1 shows the plasma wavelength of titanium-doped indium oxide films as function of the titanium doping. It can be seen that the plasma wavelength is highly dependent on the titanium doping concentration. The inset graph in Fig. 1 shows the transmission (normalized to glass) and reflection spectra as function of wavelength for a 2.3 at. % (T only) and 6.0 at. % Ti doped In_2O_3 film with a thickness of approximately 250 nm. From the spectra, it can be seen that the transmission is high (>85%) for wavelengths from about 400 nm to approximately 1750 nm. It can clearly be seen that the transmission window does change significantly with a change in titanium doping. Generally, indium oxide films sputtered in a pure argon environment have a lack of oxygen in the film and therefore a dark appearance and poor optical properties. The combinatorially sputtered titanium-doped indium oxide films, however, do have good optical properties and do not show this darkening.

The plasma wavelength determines the long-wavelength transparency limit. Figure 1 indicates that at minimum, titanium-doped indium oxide is transparent to at least 1.75 μm for the titanium composition range studied. For the 6.0 at. % reflection and transmission data shown in Fig. 1, the conductivity, carrier concentration, and mobility are equal to approximately $5\times10^3\ \Omega^{-1}\ cm^{-1}$, $8\times10^{20}\ cm^{-3}$, and $38\ cm^2\ V^{-1}\ s^{-1}$, respectively, as determined by Hall probe. With the excellent transparency and electrical properties this TCO should be very useful for applications in the visible and the near infrared.

X-ray diffraction analysis of the Ti-doped In_2O_3, as shown in Fig. 2, shows that the material is essentially crystalline In_2O_3. The XRD spectra peak locations match those of pure In_2O_3 perfectly, as also shown in Fig. 2. The XRD spectrum shows similarities to the expected powder pattern peak intensities, which would suggest that the film is essentially not textured. However, the XRD spectrum shown is obtained by integrating the raw detector images (see inset Fig. 2) along the spherical χ axis. The raw detector images clearly show that the material is actually textured (222) and that the main axis is shifted approximately 10° with respect to the χ=0° axis with a FWHW in the χ direction equal to 14°. This non-normal texture is likely due to the deposition geometry used. The logarithmic detector image shows that the texturing is less pronounced for the other crystal orientations.

A slight decrease in the absolute XRD peak height (not shown) is observed with increasing titanium doping, which may indicate that the material is becoming slightly less crystalline. No XRD spectra peak shifts were observed as function of the titanium doping concentration. This is an indication that titanium atoms substitute for indium atoms in the In_2O_3 lattice without significantly affecting the lattice constant. The fact that titanium ions (0.74 Å) are smaller than indium ions (0.94 Å) makes this possible. Similar lattice behavior has been observed in the case of zinc-doped In_2O_3, where no significant change in lattice constant is observed for low zinc doping[12] (<10%). In the reverse case of indium-doped ZnO, even for small concentrations of indium[12] (<4%) a clear change in the lattice constant can be observed since indium is significantly larger than zinc (0.88 Å).

Figure 3 shows the electrical properties (mobility, conductivity, and carrier concentration) measured by Hall probe

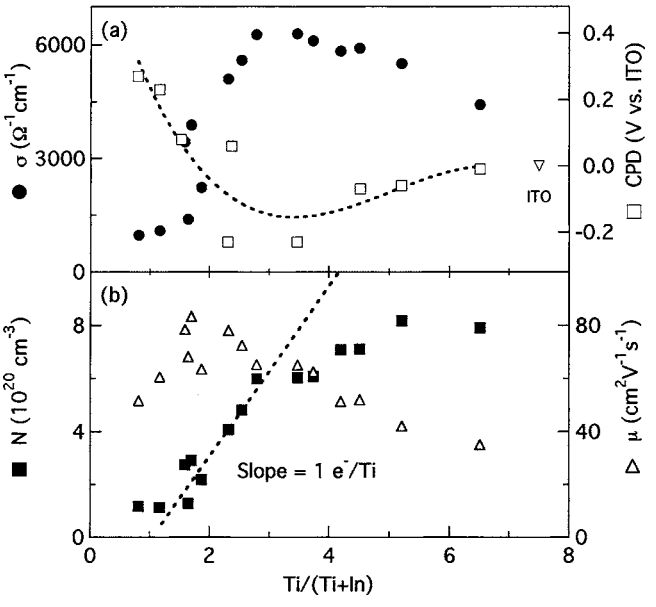

FIG. 3. (a) Conductivity σ and CPD. (b) Mobility μ and carrier concentration N of ITiO as function of titanium content obtained by EPMA.

for libraries sputtered at 550 °C covering a titanium content of 0–7 at. %, as measured by EPMA. Sputtering conditions (target powers) were chosen such as to achieve good overlap in composition between the various libraries. No discontinuities in the data are observed where the libraries overlap, indicating that the electrical properties of the deposited material are reproducible even though the location on the sample might be completely different. A maximum in the conductivity of 6260 $\Omega^{-1}\,cm^{-1}$ with a mobility of 65.1 $cm^2\,V^{-1}\,s^{-1}$ is obtained at titanium doping of approximately 2.8 at. %. A maximum in the mobility of 83.3 $cm^2\,V^{-1}\,s^{-1}$ with a conductivity of 3850 $\Omega^{-1}\,cm^{-1}$ is observed at titanium doping of 1.7 at. %. As the titanium doping increases, at first the mobility increases and then gradually falls off; simultaneously, the carrier concentration rises smoothly across the whole composition range. This results in the conductivity being low at low titanium concentration (low mobility, low carrier concentration) then rising precipitously until it remains fairly constant with the increasing carrier concentration compensating for the falling mobility. The slope of the carrier concentration in the range from 1% to 3% is equal to one carrier per substituted titanium.

In Fig. 3, it can also be seen that for titanium doping in the range from 2.5 to 6.0 at. %, the conductivity of the obtained material is above 5000 $\Omega^{-1}\,cm^{-1}$. The compositional tolerance for high conductivity material is therefore quite broad, which makes this material a very good candidate for industrial applications. Note that although the conductivity does not change drastically in the range from 2.5 to 6.0 at. %, the mobility, as well as the carrier concentration, does change by more than 50%.

Previous single composition studies of titanium-doped In_2O_3 show similar values for the optimal conductivity. Delahoy *et al.*[9] demonstrated a conductivity of approximately 5500 $\Omega^{-1}\,cm^{-1}$ for films deposited using a hollow cathode discharge. Howson *et al.*[11] were able to deposit titanium-doped In_2O_3 (1.55 at. %) films with a conductivity as high as 2200 $\Omega^{-1}\,cm^{-1}$ by means of alternate sputtering of metallic indium in a reactive atmosphere and titanium in an inert atmosphere. Note that the conductivity obtained by Howson *et al.* obtained is comparable to that of our material at similar titanium concentration.

The best conductivity of Ti-doped In_2O_3 is similar to that of the best Sn-doped In_2O_3. However the mobility for tin-doped indium oxide is lower ($\sim$30 $cm^2\,V^{-1}\,s^{-1}$) and therefore carrier concentration is higher ($\sim 10^{21}\,cm^{-3}$), resulting in less long-wavelength transparency. For Mo-doped In_2O_3, Meng *et al.*[5,6] were the first to report a similar conductivity of 5900 $\Omega^{-1}\,cm^{-1}$ with mobility around 80 $cm^2\,V^{-1}\,s^{-1}$ for 4 at. % Mo-doped In_2O_3. They initially suggested that the high conductivity and high mobility are due to the substitution of In^{3+} by Mo^{6+}. More recently, Warmsingh *et al.*[7] showed that, in fact, the electrically active molybdenum is not in the 6+ state but in the 4+ state. For molybdenum doping, approximately one carrier per four Mo atoms has been observed,[7] and for tin doping at best one carrier per two Sn atoms has been observed.[15] In contrast, we observed one carrier per Ti atom. This agrees with a classic picture of substitutional doping of In_2O_3, wherein one Ti^{4+} substitutes for one In^{3+}. Overall the Sn-, Mo-, and Ti-doped indium oxide, when optimized, produce comparable conductivities. The Ti does so over a broader composition range.

For many applications, such as organic solar cells and organic light-emitting diodes, it is important that the band edges of the various components match up. In Fig. 3(a), the contact potential difference (CPD) of ITiO is shown as a function of the titanium content. The contact potential difference as measured by the Kelvin probe can be related directly to the relative work function. The vacuum level of the work function would be of scale above the top of Fig. 3(a). Comparison of the CPD with the conductivity data shown in Fig. 3(a) shows that there is a correlation between the CPD and the conductivity. As the conductivity increases the CPD decreases. The CPD for ITiO is comparable to that of ITO, as indicated by the upside down triangle in Fig. 3(a). The CPD varies by as much as 0.5 V for different Ti concentrations. This tunability of the work function without large changes in conductivity for ITiO indicates a high potential for application as a TCO in organic solar cells.

In conclusion, it has been demonstrated that titanium-doped In_2O_3 is an excellent transparent conductive oxide. It has good electrical conductivity (6260 $\Omega^{-1}\,cm^{-1}$) for titanium doping of 2.8 at. %. In a wide range (2.5–6.0 at. %) of titanium doping the conductivity is $>$5000 $\Omega^{-1}\,cm^{-1}$. High mobility ((83.3 $cm^2\,V^{-1}\,s^{-1}$) is obtained at titanium doping of 1.7 at. %. The optical transparency is high ($>$85%) in the wide spectral range of 400 to at least 1750 nm and the work function of ITiO is highly tunable. The various properties of ITiO make it an interesting material for a large variety of applications.

The authors would like to thank Bobby To, Lynn Gedvilas, and Bonnie Mclaughlin for performing the EPMA, FTIR, and CPD measurements, respectively. The authors also would like to acknowledge the National Center for Photovoltaics sponsored by the Department of Energy and the United States Air Force for supporting this project.

[1] D. S. Ginley and C. Bright, MRS Bull. **25**, 15 (2000).
[2] T. Minami, MRS Bull. **25**, 38 (2000).
[3] A. El Hichou, A. Kachouana, J. L. Bubendorff, M. Addau, J. Ebothe, and M. Troyon, Thin Solid Films **458**, 263 (2004).
[4] M. Yamaguchi, A. Ide-Ektessabi, H. Nomura, and N. Yasui, Thin Solid Films **447–448**, 115 (2004).
[5] Y. Meng, X. Yang, H. Chen, J. Shen, Y. Jiang, Z. Zhang, and Z. Hua, Thin Solid Films **394**, 219 (2001).
[6] Y. Meng, X. Yang, H. Chen, J. Shen, Y. Jiang, Z. Zhang, and Z. Hua, J. Vac. Sci. Technol. A **20**, 288 (2002).
[7] C. Warmsingh, Y. Yoshida, D. W. Readey, C. W. Teplin, J. D. Perkins, L. M. Gedvilas, B. M. Keyes, and D. S. Ginley, J. Appl. Phys. **95**, 3831 (2004).
[8] Y. Yoshida, T. A. Gessert, C. L. Perkins, and T. J. Coutts, J. Vac. Sci. Technol. A **21**, 1092 (2003).
[9] A. E. Delahoy, L. Chen, B. Sang, S. Y. Guo, J. Cambridge, F. Ziobro, R. Govindarajan, S. Kleindienst, and M. Akhtar, Proc. of the 19th European PVSEC, Paris, 7–11 June 2004.
[10] I. Safi and R. P. Howson, Thin Solid Films **343–344**, 115 (1999).
[11] R. P. Howson, A. G. Spencer, K. Oka, and R. W. Lewin, J. Vac. Sci. Technol. A **7**, 1230 (1989).
[12] M. P. Taylor, D. W. Readey, C. W. Teplin, M. F. A. M. van Hest, J. L. Alleman, M. S. Dabney, L. M. Gedvilas, B. M. Keyes, B. To, J. D. Perkins, and D. S. Ginley, Meas. Sci. Technol. **16**, 90 (2005).
[13] C. W. Teplin, M. F. A. M. van Hest, M. Dabney, C. L. Perkins, L. M. Gedvillas, B. To, P. A. Parilla, B. M. Keyes, J. D. Perkins, D. S. Ginley, Y. Lin, and Y. Lu, Appl. Surf. Sci. **223**, 253 (2004).
[14] J. D. Perkins, C. W. Teplin, M. F. A. M. van Hest, J. L. Alleman, X. Li, M. S. Dabney, B. M. Keyes, L. M. Gedvillas, D. S. Ginley, Y. Lin, and Y. Lu, Appl. Surf. Sci. **223**, 124 (2004).
[15] J. H. Hwang, D. D. Edwards, D. R. Kammler, and T. O. Mason, Solid State Ionics **129**, 135 (2000).